Science of the Total Environment 795 (2021) 148646

Contents lists available at ScienceDirect

Science of the Total Environment

journal homepage: www.elsevier.com/locate/scitotenv

Acute hypoxia effects on Keap1/Nrf2 (Mafs)-GST pathway related oxidative metabolism in muscle of Japanese flounder (*Paralichthys olivaceus*)

Binghua Liu, Haishen Wen, Xiaohui Li, Jun Yang, Guangling Li, Meizhao Zhang, Jifang Li, Feng He *

Key Laboratory of Mariculture, Ocean University of China, Ministry of Education, Qingdao 266003, PR China

HIGHLIGHTS

- Hypoxia caused changes of epigenetic methylation modified status.
- Hypoxia affected Keap1/Nrf2 (Mafs)-GST pathway related oxidative metabolism.
- Both epigenetics and transcription factors influenced stress response regulation.
- Proteins interaction (Keap1 and Nrf2, Nrf2 and MafG) was identified in antioxidation.
- The transcriptional activation binding sequence of Nrf2 on GST promoter was explored.

GRAPHICAL ABSTRACT

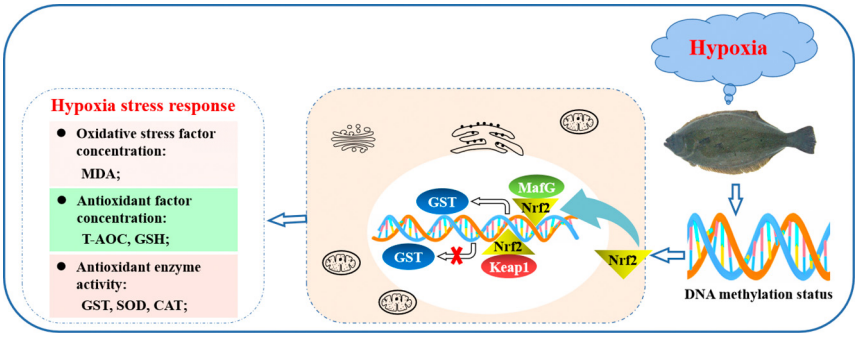

ARTICLE INFO

Article history:
Received 19 April 2021
Received in revised form 18 June 2021
Accepted 20 June 2021
Available online 1 July 2021

Editor: Henner Hollert

Keywords:
Hypoxia stress
DNA methylation
Transcriptional regulation
Antioxidation
Flatfish

ABSTRACT

Acute hypoxia can aggravate the oxidation metabolism of fish muscle tissue. However, the molecular mechanism of oxidative metabolism in fish muscle under acute hypoxia is not very clear. We carried out effects of a typical oxidative metabolism pathway Keap1/Nrf2 (MafG)-GST on muscle oxidative metabolism of Japanese flounder (*Paralichthys olivaceus*) during acute hypoxia stimulation (1.65 ± 0.05 mg/L; 1 h, 3 h, 6 h, 12 h, 24 h) and reoxygenation (7.30 ± 0.08 mg/L; R12 h, R24 h, R48 h). The mRNAs of *Nrf2* and *GST* in skeletal muscle were found coexistent, and their expressions were significant increase in 3 h and 6 h. The methylation level of CpG island1 in *Nrf2* promoter, whose minimum value appeared at 3 h hypoxia treatment group, was affected by acute hypoxia, and it was negatively correlated with *Nrf2* expression. The result suggests that environmental factors may regulate gene expression by epigenetic modification. Dual-luciferase reporter assay showed that *GST* gene was activated by transcription factor Nrf2, whose transcriptional activation binding region in *GST* promoter was antioxidant response element located near −980 and −852 sites, and Keap1 and MafG were Nrf2 antagonistic and synergistic factor, respectively. Furthermore, the GST activity changed with hypoxia and reoxygenation treatment in muscle, where other oxidative stress factor (MDA), antioxidant factors (T-AOC, GSH) and antioxidant enzyme activities (GST, SOD, CAT) were also changed. The results of MDA and T-AOC being further different between its hypoxia and normoxia groups ($P < 0.05$) at 6 h demonstrated that hypoxia stimulation lasting for 6 h would deeply affect Japanese flounder. The study illustrated that Japanese flounder responded to acute hypoxia in multiple metabolic levels by changing methylation status and transcription factor activation. It is significant to understand oxidative metabolic mechanism, analyze organism stress response and promote the scientific development of aquaculture.

* Corresponding author at: Ocean University of China, No 5 Yushan Road, Qingdao 266003, PR China.
E-mail address: hefengouc@ouc.edu.cn (F. He).

https://doi.org/10.1016/j.scitotenv.2021.148646
0048-9697/

1. Introduction

Oxygen is an important substrate for the normal life activity of most organisms. However, organisms, especially aquatic organisms, often suffer from hypoxia. When environmental factors for instance drought, osmotic stress, pH, temperature, humidity and circadian rhythm of surrounded organisms change rapidly or slowly, there will be stress response in many processes of tissue, cell, and molecule (Everis and Betts, 2001; Lin et al., 2009; Shinozaki and Yamaguchi-Shinozaki, 2007; Shu et al., 2015). Of course, it is unexceptional of hypoxia, which can decrease respiration rate and heart rate in mammals (Singer, 1999) and increase adrenaline and calcium level in freshwater turtles (Overgaard et al., 2007). Hypoxia usually induces reactive oxygen species (ROS), which would damage DNA to initiate and promote tumorigenesis, to regulate intracellular signal transduction (Canli et al., 2017; Nordberg and Arnér, 2001). Organisms resist these adverse effects by antioxidant factors, antioxidant enzymes.

Environmental stress enhances or weakens some metabolic intensities by turning on or off corresponding metabolic pathways in organisms. The regulatory grades were divided into process regulation and material regulation, in which the former includes the regulation of pre-transcription, transcription, post-transcription, translation and post-translation level; the latter includes the regulation of chromatin (DNA), RNA and protein level. The concrete patterns of material regulation contain gene rearrangement, gene amplification, DNA methylation or acetylation modification, RNA alternative splicing, protein folding, enzyme activity change, transcriptional activation or inhibition (Bird, 2002; Evans et al., 2007; Huang et al., 2018b; Ishii et al., 2002). Most of these regulatory forms are realized by signal transduction pathways including Kelch-like ECH-associated protein 1 (Keap1)/nuclear factor erythroid 2 related factor 2 (Nrf2)-antioxidant responsive element (ARE) pathway, which is a typical oxidative metabolism pathway to balance the peroxidation and anti-oxidation metabolism (Kaspar et al., 2009; Yan et al., 2019). Nrf2, belonging to Cap'n'collar (CNC) family, as a transcription factor, can translocate into nuclei to activate its downstream target genes for example anti-oxidation genes, such as heme oxygenase-1 (*HO-1*), NAD(*P*)H: quinone oxidoreductase (*NQO1*), glutathione S-transferases (*GST*), and glutamate-cysteine ligase (*GCL*), whose promoters contain one or more ARE, whose core sequence is TGACNNNGC (Hirotsu et al., 2012; Innamorato et al., 2008; Ke et al., 2013; Lee et al., 2003; Sykiotis and Bohmann, 2010). Furthermore, here is a kind of Nrf2 dimerization partner musculo aponeurotic fibrosarcoma (Maf) proteins (MafS), including MafA, MafB, MafF, MafG and MafK, which are leucine zipper proteins but lack transcription activation domains, that can assist Nrf2 to activate target genes (Artner et al., 2010; Blank, 2008; Hirotsu et al., 2012; Rahman et al., 2013). However, Nrf2 would be retained in cytoplasm and is difficult to perform the activated function by its inhibitor (INrf2) which include Keap1 (Kaspar et al., 2009).

Multiple signaling pathways, which cascade amplification step by step, are composed of signal-transduction network (Nakabayashi and Sasaki, 2005). Signal regulation, whose results can be shown as the changes of mRNA expression, protein content, enzyme activity, leads to changes in the interaction between various biomolecules and affects ultimately phenotype. For example, lncRNA-NUTF2P3-001 was induced by hypoxia to depress miR-3923/KRAS pathway to contribute to tumorigenesis of pancreatic cancer (Li et al., 2016); the expression levels of AMPK pathway related factors were changed to maintain energy homeostasis in olive flounders when suffered from low-temperature stress (Lu et al., 2018).

However, the antioxidant metabolism regulatory mechanism from micro-molecular to macro-phenotype has not been fully understood. Because oxygen content in water is 1/30th that of same volume air, and the diffusion rate is only 1/10000th that in air, aquatic organisms are model organisms for studying hypoxia stress response (Rytkönen et al., 2007). Therefore, we conducted an acute hypoxia [1 h (hour), 3 h, 6 h, 12 h, 24 h] and reoxygenation (R12 h, R24 h, R48 h) treatment on Japanese flounder (*Paralichthys olivaceus*). Japanese flounder is an important economic benthic marine fish, which is widely cultivated in the Japan, Korea and China (Cabrera and Hur, 2001; Fuji et al., 2007). Liking other fishes, its growth is affected by environmental factors (temperature, dissolved oxygen, nutrition, and stocking density, etc) and biological factors (virus and predator, etc) (Cabrera and Hur, 2001; Duan et al., 2011; Miyazaki et al., 2004; Seikai et al., 1986; Wang et al., 2021). Therefore, we focused on Japanese flounder as the experimental object to research the mechanism of hypoxia response and adaption. It was changed of some oxidation and antioxidant indexes levels in muscle homogenate. The molecular regulatory mechanisms of a typical antioxidant metabolic pathway Keap1/Nrf2 (Mafs)-GST, including epigenetic modification and transcription factor regulation, were explored and verified. Our study elucidated the mechanism of stress response and adaptation from micro to macro level, which could explain the relevant stress theory and guide aquaculture production.

2. Materials and methods

2.1. Ethics statement

All experimental Japanese flounder were treated in accordance with the guidelines of Animal Research and Ethics Committees of Ocean University of China, and there were no endangered species or protected species.

2.2. Hypoxic treatment and sampling

Japanese flounder were collected from Qingdao HaoRuiYuan aquaculture Co., Ltd., China. All fish were temporarily reared three days to acclimatize seawater, which was filtered and disinfected in one aquaria tank ($1.5 * 1.5 * 0.6$ m^3 with about 1000 L seawater, about 30 ind/m^2), prior to the hypoxic experiment. In acclimatization period, the seawater was changed once a day, and the environmental parameters were as follows. It was maintained at 18.5 ± 0.08 °C (range: 17.5–19.3 °C) of water temperature, 7.6 ± 0.02 (range: 7.3–7.7) of pH, 29 ± 0.06 ppt (range: 28–30 ppt) of salinity, 7.47 ± 0.03 mg/L (range: 7.06–7.91) of dissolved oxygen (DO) (YSI EcoSense DO200A dissolved oxygen meter, USA), 14 h light: 10 h dark of photoperiod. It is worth noting that about 7.5 mg/L was selected as the DO concentration in the acclimatization period, control and reoxygenation group, and its 25% (i.e. 1.875 mg/L) which is higher than half lethal DO concentration in the hypoxia treatment group (Dong et al., 2013; Duan et al., 2011; Ishibashi et al., 2007). All fish were fed twice (at 9:00 am and 3:00 pm) daily with Surgreen® commercial compound feed for marine fish (Surgreen, China), in which residual feed and feces were removed after the fish stopped eating, but fasted for 24 h before hypoxic treatment. These fish were randomly distributed to two DO treatment groups with triplicate in 6 rectangular tanks ($0.6 * 0.5 * 0.5$ m^3 with about 120 L seawater, about 30 ind/m^2), in which the half were treated by normoxia [7.43 ± 0.03 mg/L (range: 6.69–8.28)] and the remaining half by hypoxia [1.65 ± 0.05 (range: 1.10–2.08 mg/L)], which were begun to undergo reoxygenation treatment [7.30 ± 0.08 mg/L (range: 6.60–8.19)] after 24 h hypoxia stress. Except for no water changing and DO, which was maintained by pumping air or nitrogen from a steel cylinder in hypoxia treatment groups, other water parameters (temperature, pH, and salinity) were kept same as the acclimation period. The 17 groups of fish including acute hypoxic stress groups 0 h (control), 1 h, 3 h, 6 h, 12 h, 24 h, reoxygenation 12 h, 24 h, 48 h (R12 h, R24 h, R48 h) and their corresponding control groups (normoxia groups: 1 h, 3 h, 6 h, 12 h, 24 h, R12 h, R24 h, R48 h) were sampled 9 times on time. Specifically, fish were anesthetized with tricaine methane sulfonate (MS-222, 200 mg/L). The body weight ($n = 51$, 45.38 ± 1.33 g) and length (15.03 ± 0.35 cm) were measured immediately. Fishes were dissected

to obtain skeletal muscles, which were promptly frozen in liquid nitrogen, afterwards stored at −80 °C for DNA and RNA extraction and tissue homogenate preparation. In addition, some skeletal muscle tissues were fixed into 4% paraformaldehyde for double in situ hybridization (D-ISH).

2.3. Bioinformatics analysis

The analyses of gene sequence were conducted by an online software Gene Structure Display Server (GSDS 2.0) (http://gsds.gao-lab.org/index.php). In addition, presumptive transcription factors (TFs) and their binding sites on genes were predicted by JASPAR online software (http://jaspar.genereg.net/), especially Nrf2 transcription factor binding sites on *GST* genes.

We analyzed the physical and chemical characteristics of these four proteins (Keap1, Nrf2, GST, MafG). The molecular weight and theoretical isoelectric point (pI) of these proteins were predicted by the ProtParam tool online software (https://web.expasy.org/protparam/). The online software of Simple Modular Architecture Research Tool (SMART) (http://smart.embl.de/) and TMHMM Server v. 2.0 (http://www.cbs.dtu.dk/services/TMHMM/) were used to predict the domains and transmembrane helices number, respectively. Furthermore, preliminarily proteins three-dimensional structures were predicted by SWISS-MODEL online software (https://swissmodel.expasy.org/interactive) and depicted deeply by PyMOL 2.3.2 software.

The protein (Keap1, Nrf2, GST and MafG) evolutionary relationships of Japanese flounder with other species were analyzed by constructing phylogenetic trees, which were constructed using Molecular Evolutionary Genetics Analysis software (MEGA 7.0) with Neighbor-Joining (NJ) method (under 1000 bootstrap replications).

2.4. Quantitative real-time PCR and expression analysis

RNA isolater Total RNA Extraction Reagent (Vazyme, China) was used to extract total RNA from skeletal muscle. Nucleic acid analyzer Biodropsis BD-1000 (OSTC, China) was used to measure RNA concentration, agarose gel electrophoresis to RNA integrity. Afterwards, cDNA was obtained by using HiScript® III RT SuperMix for q-PCR (+gDNA wiper) (Vazyme, China), and quantitative real-time PCR (q-PCR) was conducted by using an Applied Biosystems StepOne Plus Real-Time PCR System (Applied Biosystems, USA) with ChamQ™ SYBR® Color q-PCR Master Mix (High ROX Premixed) (Vazyme, China). Here, mRNA relative expressions of *Keap1*, *Nrf2*, *GST* and *18S* (as internal reference) were determined by q-PCR, in which all primers (Table S1A) [except for *18S* primers, which was referred to Wu et al., 2018] were designed by Primer Premier 5 software (Premier, Canada) and were detected specifically by Primer-BLAST (https://www.ncbi.nlm.nih.gov/tools/primer-blast/). In detail, the q-PCR system (10 μL) contains 2 × ChamQ SYBR Color q-PCR Master Mix (High ROX Premixed) 5 μL, Forward Primer (F) 0.2 μL, Reverse Primer (R) 0.2 μL, cDNA template (4 × diluted) 1 μL, and ddH_2O 3.6 μL. All samples were repeated in triplicate as technical replicates. The q-PCR procedure was 95 °C for 30 s, 40 cycles of 95 °C for 10 s, annealing temperature which was showed in Table S1A for 30 s. The relative expressions were calculated according to the comparative threshold ($2^{-\Delta\Delta Ct}$) method.

2.5. DNA methylation level detection

According to the changing trend of *Nrf2* gene relative expression, five groups (0 h, 3 h, 6 h, 12 h, R12 h) were chosen to detect its promoter methylation level. Genome DNA, which was extracted from skeletal muscle by using FastPure® Cell/Tissue DNA Isolation Mini Kit (Vazyme, China), was modified by bisulfite [BisulFlash™ DNA Modification Kit (EpiGentek, USA)]. The 2 × EpiArt™ HS Taq Master Mix Kit (Vazyme, China) was used subsequently to conduct methylation-specific PCR (MS-PCR), in which primers (Table S1B) were designed and CpG islands were predicted by online MethPrimer design software (http://www.urogene.org/methprimer/). The purified DNA sequence [FastPure® Gel DNA Extraction Mini Kit (Vazyme, China)] in MS-PCR was connected with pEASY-T1 vector (TransGen, China) to construct promoter sequence contained plasmid, which was transferred into DH5α competent cell (Vazyme, China) subsequently. Three biological repetitions in each treatment group and about 10 clones in each fish were followed. In addition, it was calculated of the percentage of converted cytosines (excluding cytosines of CpG dinucleotides), which was equal to [number of converted cytosines (excluding cytosines of CpG dinucleotides)] / [total number of cytosines (excluding cytosines of CpG dinucleotides)] × 100, to evaluate bisulfite modification efficiency and experimental results credibility.

2.6. Double in situ hybridization of Nrf2 and GST RNA in skeletal muscle

Muscle tissue frozen sections were obtained according to Kanda et al. (2011) with minor modifications. Briefly, skeletal muscle tissue was fixed into 4% paraformaldehyde solution, dehydrated in 30% sucrose solution, reversed water with 50%, 75%, 100% PBS in turn, embedded in OCT embedding agent (SAKURA, Japan). Afterwards, a tissue slicer (LEICA TP-1020, Germany) was used to obtain muscle tissue slices (thickness = 7 μm).

The objective DNA sequences of *Nrf2* (512 bp) and *GST* (474 bp) genes were amplified from cDNA template by high fidelity PCR (Phanta® Max Super-Fidelity DNA Polymerase Kit, Vazyme, China), in which the primers (Table S1C) were added three protective bases-SP6 promoter sequence (cgc-atttaggtgacactatagaagcg) or T7 promoter sequence (ccg-taatacgactcactatagggagaca) in the 5′ end of forward primer or reverse primer, respectively, after they were designed by Primer Premier 5 software. The objective DNA sequences were purified as DNA template in transcription by FastPure® Gel DNA Extraction Mini Kit (Vazyme, China) after agarose gel electrophoresis separate. In the transcription system, 1 μg DNA template, 2 μL 10*RNA Polymerase Reaction Buffer (NEB, USA), 1 μL Ribonuclease Inhibitor (TRANS, China), 2 μL T7 RNA Polymerase (Roche, Switzerland), 2 μL 10*NTP and RNase free H_2O were mixed to the volume of 20 μL. It is necessary to note that *Nrf2* probes and *GST* probes were transcribed by digoxigenin (DIG) labeled NTP (DIG RNA Labeling Mix 10* conc, Roche, Switzerland) and Biotin labeled NTP (Biotin RNA Labeling Mix 10* conc, Roche, Switzerland), respectively. Then we manipulated DIG or Biotin labeled RNA probe and target RNA hybridization experiment, whose method was consistent with that in Kanda et al. (2011) and Li et al. (2020) paper.

2.7. Dual-luciferase reporter assay

Here, the *GST* gene regulated by transcription factor Nrf2 was verified by dual-luciferase reporter assay. First, we chose pcDNA 3.1(+) plasmid and single restriction endonuclease [BamHI (NEB, USA)] or double restriction endonuclease [*Hin*dIII and BamHI (NEB, USA)] to construct expression plasmid (pc3.1 ~ Nrf2, pc3.1 ~ MafG, pc3.1 ~ Keap1), similarly, pGL3-Basic plasmid and double endonuclease [*Xho*I, HindIII (NEB, USA)] to construct *GST* gene reporter plasmid (G ~ pGL). Specifically, *Nrf2* CDS and *GST* promoter sequences were obtained by high-fidelity PCR, in which primers (Table S1D) sequences were added restriction sites and homologous sequences of corresponding plasmids in 5′ end. Secondly, ClonExpress® Ultra One Step Cloning Kit (Vazyme, China) was used to connect linearized plasmid, which was digested by corresponding restriction endonuclease and purified, and CDS or promoter sequence to obtain homologous recombinant plasmids. The plasmid was transferred into DH5α chemically competent cell (Vazyme, China) to obtain monoclonal cells, which were sequenced [Beijing Genomics Institute (BGI), China] after culturing in ampicillin resistant Luria-Bertani (LB) medium. EndoFree Mini Plasmid Kit II (TIANGEN, China) was used to extract the plasmids which were

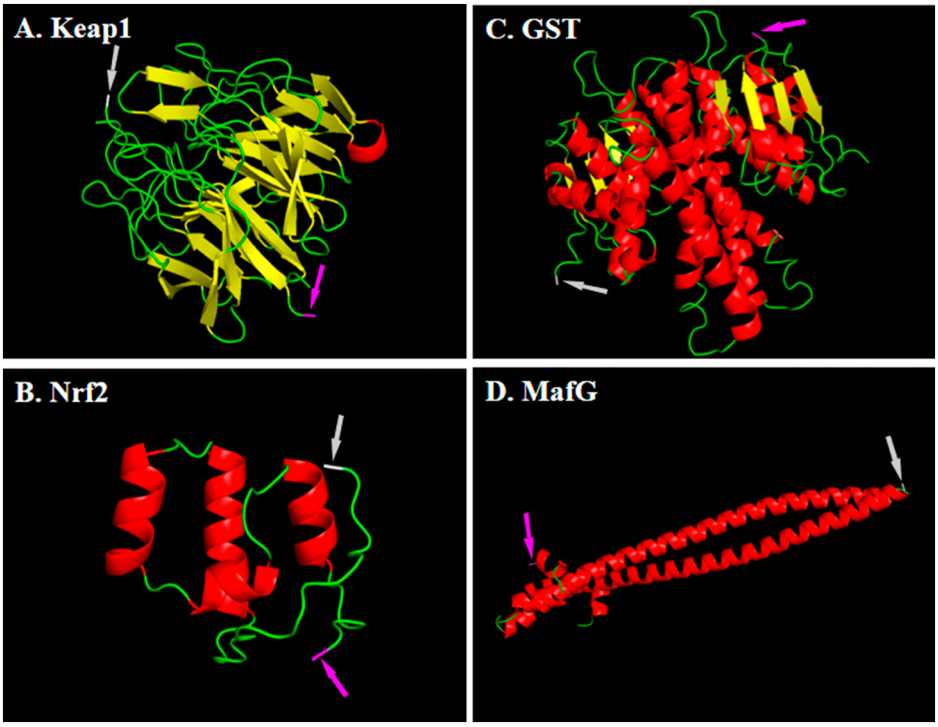

Fig. 1-1. The three-dimensional structures of Keap1 (A), Nrf2 (B), GST (C) and MafG (D) protein in Japanese flounder. The N-term and C-term are labelled with magenta arrows and gray arrows, respectively. The α helices, β sheets and loop are colored in red, yellow and green, respectively.

sequenced to meet requirements from bacterial fluid. Thirdly, plasmids were transfected into human embryonic kidney 293T (HEK293T) cells. In detail, HEK293T cells, which were cryopreserved in liquid nitrogen, were resuscitated (37 °C) and cultured to 3th or 4th generation, whose growth was normal and steady. Subsequently, cells were placed in 24 well plates (Corning, USA) at the concentration of 10^5 cells per well. When the confluence of cells reached 50% to 70%, plasmids were transfected into HEK293T cells by strictly following the instructions of Xfect™ Transfection Reagent Kit (Takara, Japan), in which pRL-TK (Promega, USA) was used as control plasmid to express Ranilla luciferase to detect the transfection efficiency. The DMEM culture medium (Spark Jade, China) with 10% foetal bovine serum (FBS) (BioInd, Israel) was changed 4 h after transfection. Fourthly, SYNERGY HTX multi-mode reader (BioTek, USA) was used to measure the double-fluorescence values after transfection 48 h by Dual-Luciferase kit (Promega, USA), whose instruction was strictly followed.

In addition, in order to test the specific binding sites of transcription factor Nrf2, fragment deletion and directed base sites mutation of *GST* gene promoter were carried out based on the previous series of results to construct reporter plasmids, including G3 ~ pGL, G2 ~ pGL, G1 ~ pGL, G0 ~ pGL which belong to fragment deletion reporter plasmids

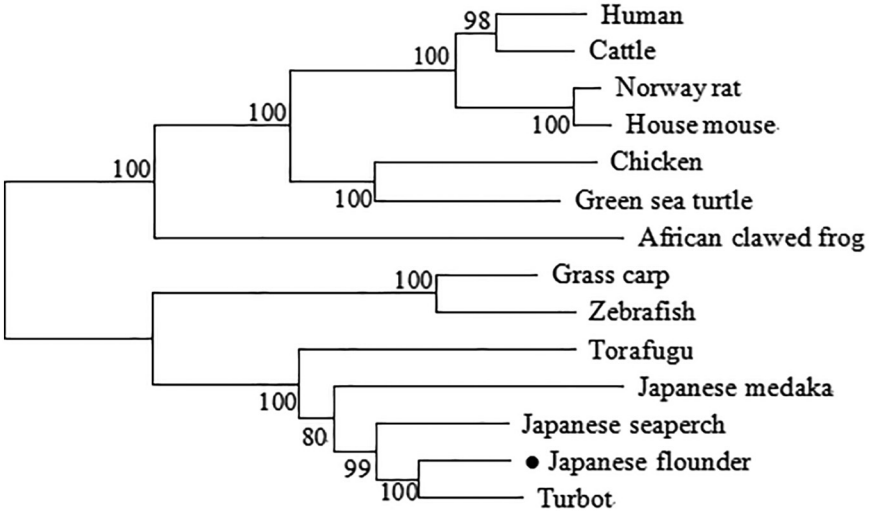

Fig. 1-2. Phylogenetic trees of Nrf2. The site of Japanese flounder is marked with solid black dot. The accession numbers of Nrf2 protein in different species are as follows. Japanese flounder (*Paralichthys olivaceus*): XP_019945790.1; Human (*Homo sapiens*): AAB32188.1; Grass carp (*Ctenopharyngodon idella*): ART92576.1; Norway rat (*Rattus norvegicus*): NP_113977.1; Zebrafish (*Danio rerio*): BAC10573.1; House mouse (*Mus musculus*): NP_035032.1; Cattle (*Bos taurus*): NP_001011678.2; Japanese aperch (*Lateolabrax japonicus*): AMS75114.1; African clawed frog (*Xenopus laevis*): NP_001086307.1; Chicken (*Gallus gallus*): QIQ56209.1; Japanese medaka (*Oryzias latipes*): XP_004081819.1; Torafugu (*Takifugu rubripes*): XP_003961876.2; Turbot (*Scophthalmus maximus*): AWP13156.1; Green sea turtle (*Chelonia mydas*): EMP35077.1.

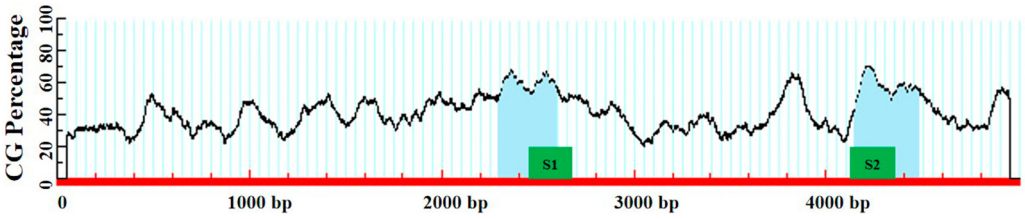

Fig. 2-1. The two CpG islands (light blue areas: CGI1, CGI2) and methylation status detecting sequences (green areas: S1, S2) in *Nrf2* gene promoter. Their sites relative to the start codon (ATG) are −2158 to −1858 (CGI1, 301 bp), −304 –+27 (CGI2, 331 bp), −1984 to −1800 (S1, 185 bp), −316 to −125 (S2, 192 bp), respectively.

and M5 ~ pGL, M4 ~ pGL, M3 ~ pGL, M2 ~ pGL, M1 ~ pGL belonging to directed bases mutation reporter plasmids. It should be noted that the promoter sequences (M5, M4, M3, M2, M1) of site mutation were obtained by fusion PCR method, whose primers sequences were also shown in Table S1D.

2.8. Detection of oxidation factors (MDA, T-AOC, GSH, SOD, GST, CAT)

Under the condition of ice-water bath, skeletal muscle (1-time mass, g) and normal saline (9-times volume, mL) were mixed in an eppendorf tube and ground fully in a Tissue Grinder (DHS, China). Then, 10% muscle tissue homogenate was obtained after centrifugation (2500 rmp, 10 min, 4 °C) and discarding sediment. It is worth mentioning that CAT activity kit (Solarbio, China) instruction was followed to obtain muscle tissue homogenate to detect catalase (CAT) activity. In addition, because many oxidation factors need protein content as a prerequisite, total protein (TP) in muscle tissue homogenate was measured by Total protein quantitative assay kit (Nanjing Jiancheng Bioengineering Institute, China). Malondialdehyde (MDA), Total antioxidant capacity (T-AOC), GSH, Superoxide Dismutase (SOD) and Glutathione S-transferase (GST) were detected with the kit produced from Nanjing Jiancheng Bioengineering Institute (China), including MDA assay kit, T-AOC assay kit, Total glutathione/Oxidized glutathione assay kit, SOD assay kit (WST-1 method), GST assay kit (Colorimetric method).

2.9. Statistical analysis

Data were presented as mean ± standard error (M ± SE). On the requirements of analytical methods being met, one-way ANOVA with Duncan's post hoc test was conducted to detect statistical differences (Tian et al., 2019), and linear regression analysis was performed to explore linear relationships between mRNA relative expression and methylation level, between mRNA relative expressions of two genes. SPSS 22.0 was used for statistical analyses, OriginPro 9.0 for making graphs. *P* value was set at 0.05, which was represented significant difference by different small letters on the columns.

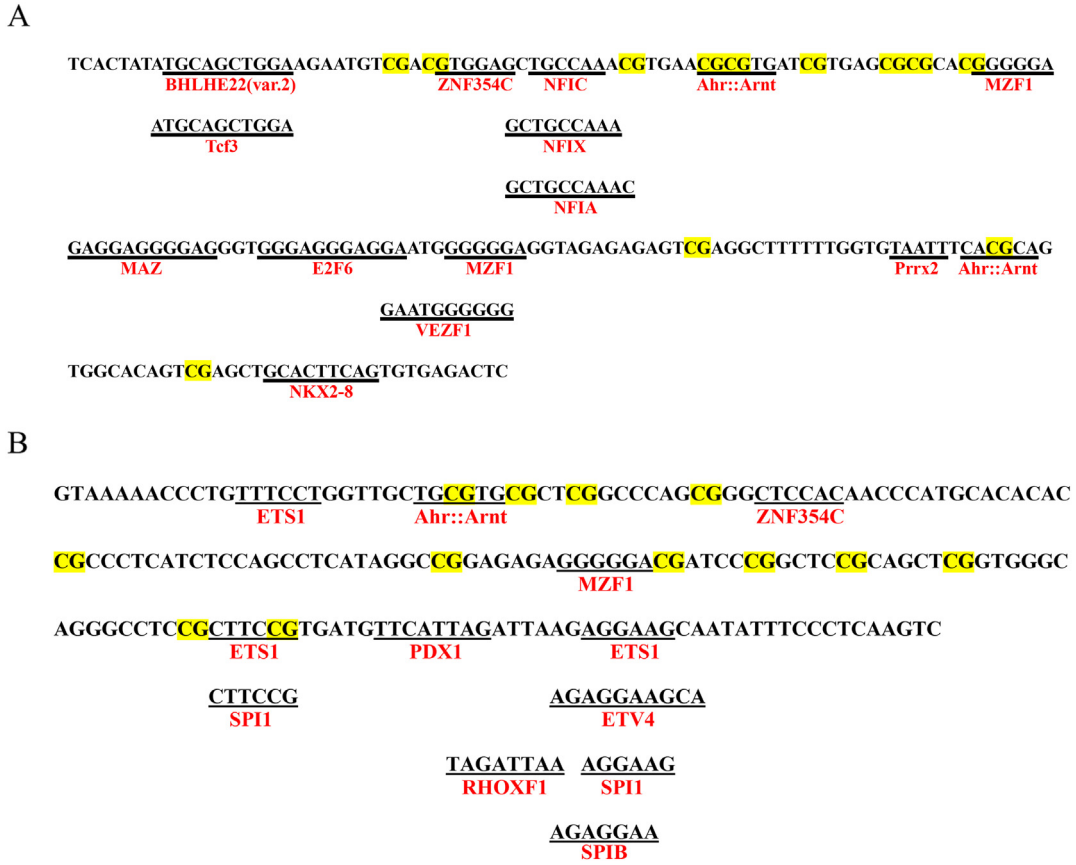

Fig. 2-2. Transcription factors (TFs) and their binding sites (95% Relative profile score threshold) in S1 (A) and S2 (B). The yellow shaded areas indicate CpG dinucleotides sites, and the letters on the black underline indicate transcription factor binding sequence. The letters under the black underline indicate TFs, which include BHLHE22(var.2), ZNF354C, NFIC, Ahr::Arnt, MZF1, Tcf3, NFIX, NFIA, MAZ, E2F6, Prrx2, VEZF1, NKX2-8 and ETS1, Ahr::Arnt, ZNF354C, MZF1, PDX1, SPI1, ETV4, RHOXF1, SPIB.

3. Results

3.1. Bioinformatics analysis

The results of gene (*Keap1*, *Nrf2*, *GST* and *MafG*) sequence analyses are shown in Fig. S1, Table S2, and protein sequence information and domain analytical results are represented in Table S3 and Fig. S2, in which there are three (BTB, BACK, Kelch), one (BRLZ), one (BRLZ) different domain in Keap1, Nrf2 and MafG protein, respectively. The three-dimensional structures of these four proteins (Keap1, Nrf2, GST and MafG) are shown in the Fig. 1-1, in which α-helix, β-sheet and loop secondary structures are found. To know the evolutionary relationship, phylogenetic trees, showing in Fig. 1-2, Fig. S3, were constructed. All trees of these four proteins are divided into two clades, whose classified into fish and other advanced vertebrates in Keap1, Nrf2 and MafG; however, fishes were divided into two branches in GST.

3.2. DNA methylation status and expression level of Nrf2 gene

Methylation levels of two sequences (S1: −1984 to −1800, 185 bp; S2: −316 to −125, 192 bp) were detected in CpG islands (CGI1: −2158 to −1858, 301 bp; CGI2: −304 –+27, 331 bp) of *Nrf2* gene promoter (Fig. 2-1). Furthermore, 15 and 12 transcription factors and their binding sites (95% Relative profile score threshold) about S1 and S2 were shown in Fig. 2-2A, B, and these transcription factors included BHLHE22(var.2), ZNF354C, NFIC, Ahr::Arnt, MZF1, Tcf3, NFIX, NFIA, MAZ, E2F6, Prrx2, VEZF1, NKX2-8 and ETS1, Ahr::Arnt, ZNF354C, MZF1, PDX1, SPI1, ETV4, RHOXF1, SPIB. We randomly selected 12 sequencing results of the S1 and S2 to calculate bisulfite modification efficiency. Only 11 cytosines (19 cytosines outside 12 CpG dinucleotides per 185 bp) were not converted to thymine in S1, indicating bisulfite modification efficiency was 95.18% [95.18% = (12 × 19–11) / (12 × 19) × 100%], which means very efficient (Fig. S4A shows part of the sequencing result). Similar highly efficient [95.26% = (12 × 51–29) / (12 × 51) × 100%] was discovered in S2 (Fig. S4B). The methylation level of S1 and S2 showed a low level overall (S1: 6.10 ± 0.64%, S2: 5.94 ± 0.91%), and their change trends first decreased and then recovered with the prolongation of hypoxia stress and reoxygenation (Fig. 2-3A, B, C). Its change in S1 was significant, however, S2 was not. Concretely, the methylation level of 3 h hypoxia group was significantly lower than that of control group (0 h), and this lower level had not recovered when hypoxia lasted for 12 h, but did recover when reoxygenation 12 h (Fig. 2-3A, B). The minimum methylation level of S2 appeared in 6 h hypoxia treatment group (4.44 ± 1.11%), but there was no significant difference among these 5 groups (Fig. 2-3A, C). Subsequently, the methylation level of the 24 CpG dinucleotides was also analyzed, and they change trends were different. Concretely, trend of rising first and then decreasing appeared at the site of −1919, −1915, −1862, −1838, −1824, −286, −282, −274, −204, −191; decreasing first and rising then at −1941, −1935, −1927, −1921, −290, −210, −175 (Fig. S5). Some decreased or increased continuously with the prolongation of hypoxia stress and reoxygenation.

The *Nrf2* mRNA relative expression, whose change trend was first increase and then decrease, was shown in Fig. 2-4. The maximum value (8.42 ± 1.72) appeared in 6 h hypoxia treatment group, which was significantly higher (3.03 times) than that of its corresponding control group. However, there was no significant difference between 24 h hypoxia group and its control group, three reoxygenation groups (R12 h, R24 h, R48 h) also no significant difference. Next, the relationships between methylation levels and expressions of *Nrf2* gene were analyzed by linear regression analysis, which showed that the *Nrf2* mRNA expressions were negatively correlated ($R = -0.815, -0.915$; $R^2 = 0.6639, 0.8377$) with the average methylation levels of these two (S1, S2) sequences (Fig. 2-5A, B). The relationships between methylation level of single CpG dinucleotides and expression were also analyzed (Table S4), in which expression was negatively with methylation level in −1941, −1927, −1921, −198 and −169 CpG site, positively in −1915 CpG site.

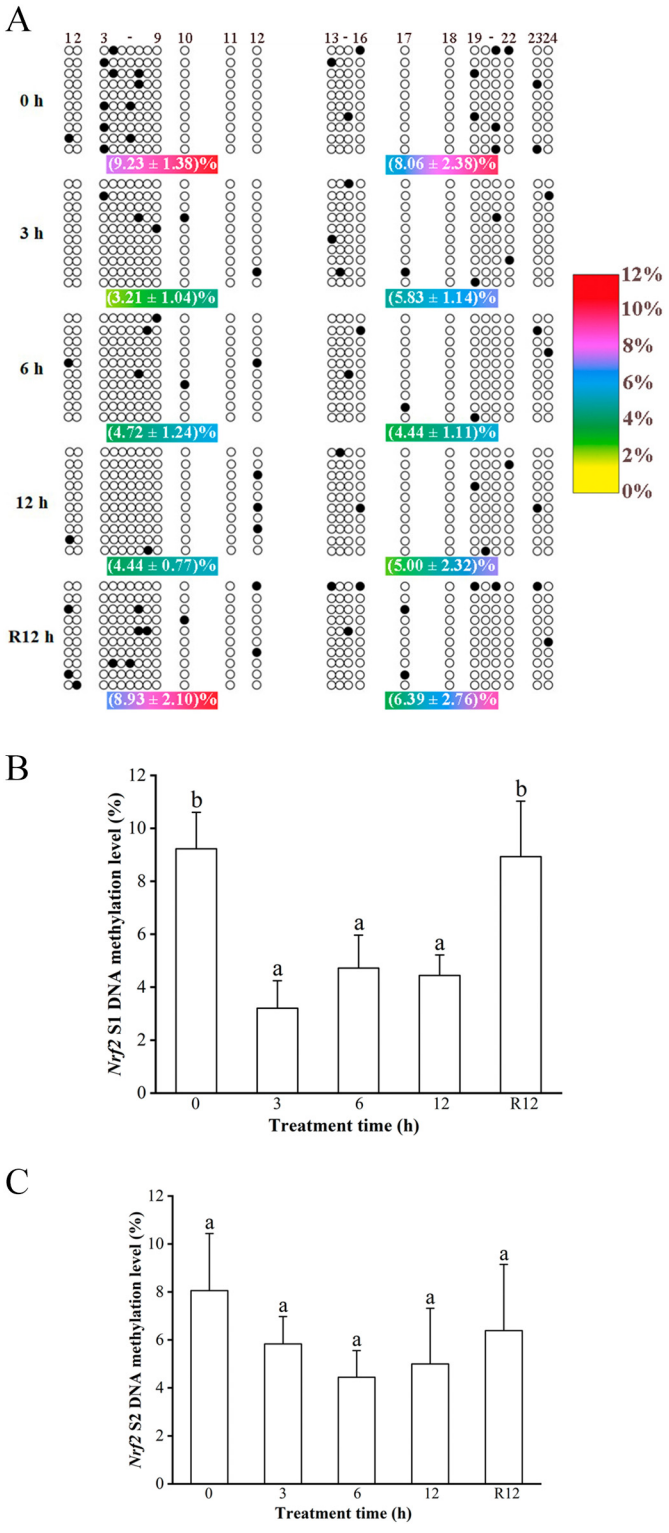

Fig. 2-3. Methylation level of *Nrf2* gene promoter at different hypoxia stress times. (A) Circles indicate methylation status, which black solid circles (●) represent methylated state, black hollow circle (○) unmethylated state. The top numbers (1–24) represent 24 CpG dinucleotides, whose sites relative to the start codon (ATG) are −1959, −1956, −1941, −1935, −1933, −1927, −1921, −1919, −1915, −1862, −1838, −1824; −290, −286, −282, −274, −249, −224, −210, −204, −198, −191, −175, −169. The percentages under circles show the methylation levels (M ± SE). It is the methylation level of S1 (B) and S2 (C) detecting area in *Nrf2* gene promoter. Different letters indicate significant differences ($P < 0.05$).

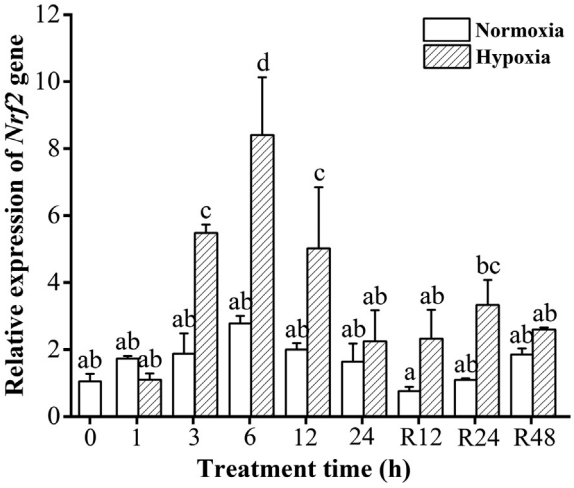

Fig. 2-4. *Nrf2* mRNA relative expression in skeletal muscle at different normoxia and hypoxia (reoxygenation) times. Different letters indicate significant differences ($P < 0.05$).

3.3. Keap1 and GST gene mRNA relative expression

Keap1 mRNA relative expressions were almost at the same level among all groups except for the 1 h treatment group (Fig. 3-1A). In contrast, relative expressions of *GST* mRNA of four treatment groups (3 h, 6 h, 24 h, R24 h) were significantly different (Fig. 3-1B).

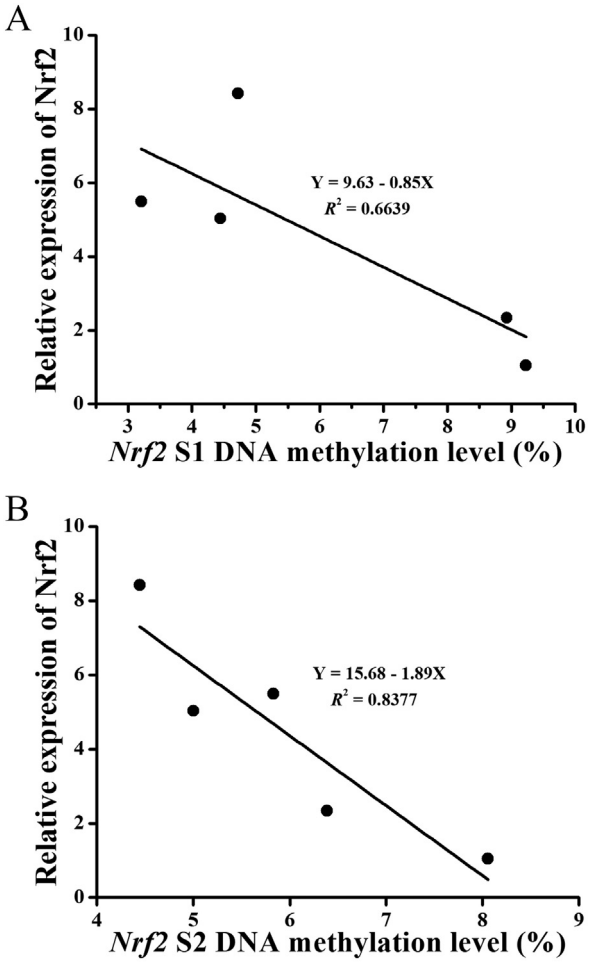

Fig. 2-5. The relationships between *Nrf2* mRNA relative expressions and methylation levels of its promoter S1 or S2 by linear regression analysis.

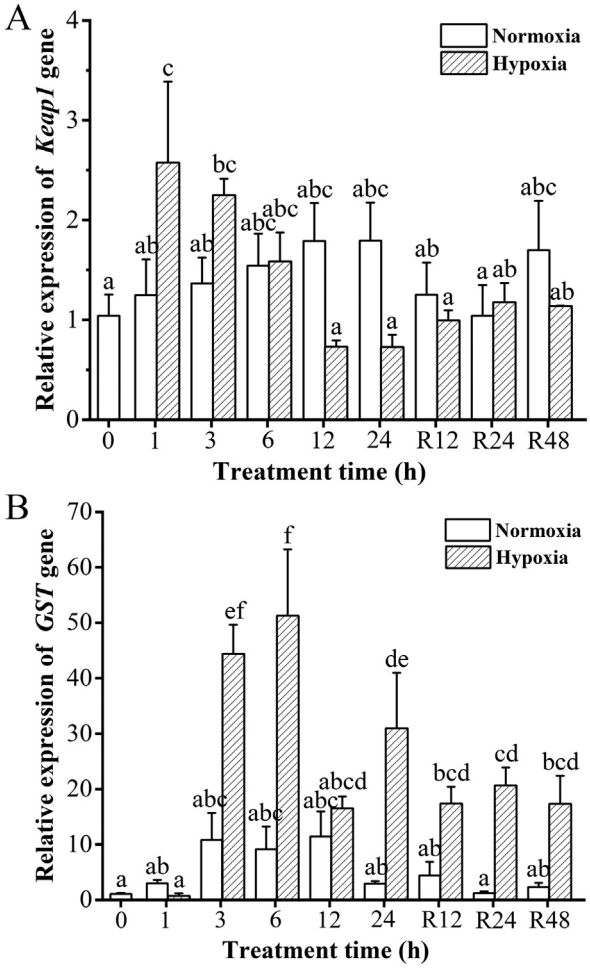

Fig. 3-1. The mRNA relative expression of *Keap1* (A) and *GST* (B) in skeletal muscle. Different letters indicate significant differences ($P < 0.05$).

Furthermore, the change trend of *GST* mRNA expression was increased first and decreased then, which was still not recovered to the control level when reoxygenation 24 h.

3.4. The regulatory relationship of Nrf2 and Keap1, GST

The correlation of mRNA relative expressions was strong positive between *GST* and *Nrf2* ($R = 0.871$, $R^2 = 0.758$), not between *Nrf2* and *Keap1* by linear regression analysis (Fig. 4-1A, B). *Nrf2* and *GST* mRNAs were located near the nucleus of muscle cells (Fig. 4-2, Fig. S7) by performing D-ISH.

Dual-luciferase reporter assay was used to further research the regulatory relationships between Nrf2 and Keap1, GST. Here, MafG, a member of MafS family, was also selected to carry out this experiment to verify whether it could assist Nrf2 activate downstream target genes. It could be seen from the Fig. 4-3A that the relative luciferase activity of the 6-group which contained expression plasmid pc3.1 ~ Nrf2 was significantly higher than that of the 5-group which only contained blank circular plasmid (pc3.1) (d Vs. b). Significant difference (c Vs. b) was also found between 7-group (contained expression plasmid pc3.1 ~ MafG) and 5-group. When expression plasmids pc3.1 ~ Nrf2 and pc3.1 ~ MafG co-transfected into HEK293T cells (8-group), luciferase activity value (15.55 ± 0.39) was significantly higher than that of other groups (e Vs. a, b, c, d). The specific binding sites of transcription factor Nrf2 were detected by the method of fragment deletion. In the Fig. 4-3B, relative luciferase activity values were different in the several groups. Concretely, the values of three fragment deletion groups (G1 ~

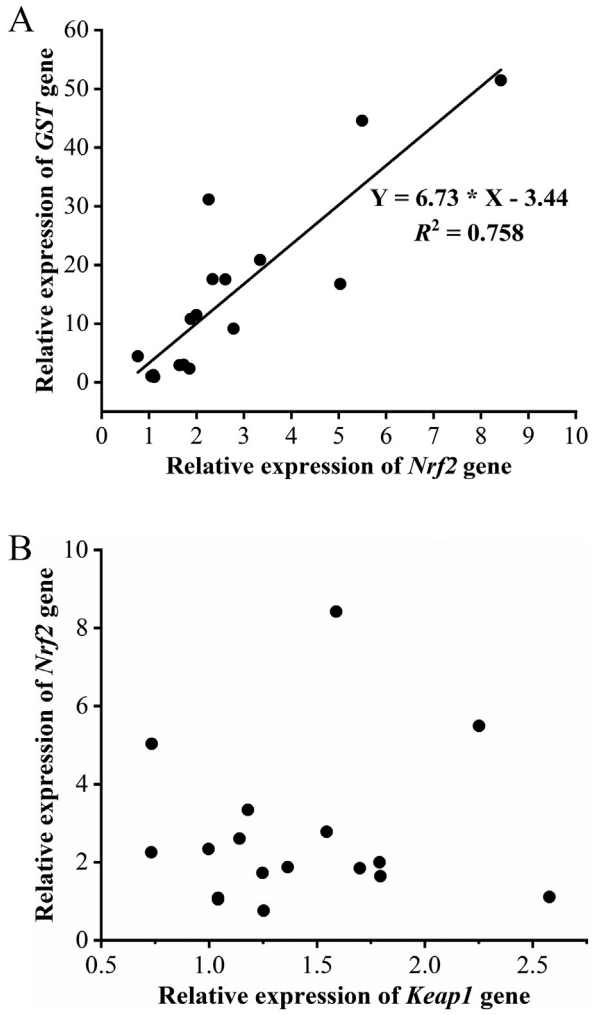

Fig. 4-1. The relationships of mRNA relative expressions between (A) *GST* and *Nrf2*, (B) *Nrf2* and *Keap1* in skeletal muscle.

pGL, G2 ~ pGL, G3 ~ pGL) were significantly higher than that of control group (pGL) (c, c, c Vs. a), and it was not dramatically lower in pGL group than that in the fragment deletion group (G0 ~ pGL) (a Vs. ab). So, the Nrf2 binding sites were likely appeared in −1160 ~ −748 (413 bp) site region. To detect whether the ARE sequences near −980 and − 852 sites, which were detected by JASPAR software, were transcription factor Nrf2 binding sites, which are concluded from Fig. 4-3B, these two sequences in their reporter plasmids were mutated to verify the conjecture. In the Fig. 4-3C, relative luciferase activity values of mutational plasmids were significantly lower than that of their corresponding control plasmids. In other words, the value of G0 ~ pGL was lower than G1 ~ pGL (cd Vs. e); M1 ~ pGL, M2 ~ pGL, M3 ~ pGL than G1 ~ pGL (bc, abc, ab Vs. e); M4 ~ pGL, M5 ~ pGL than G ~ pGL (abc, ab Vs. d). Interestingly, the relative luciferase activity value of G ~ pGL, whose promoter sequence was longer, was lower than that of G1 ~ pGL (d Vs. e). When added expression plasmid pc3.1 ~ Keap1 to transfect HEK293T cells in the 5-group which contained pc3.1 ~ Nrf2 plasmid, the relative luciferase activity value was significantly lower (a Vs. d) than its control group (2-group) (Fig. 4-4,). Similar results were found in pc3.1 ~ MafG plasmid [6-group (a) Vs. 3-group (c)].

3.5. Effect of acute hypoxia on oxidation factors

MDA is a product of lipid peroxidation that can cause membrane lipid peroxidation and cell damage. Its concentration was no significant difference in all groups except for the 6 h group, in which it was significantly higher in hypoxia than that in normoxia treatment (Fig. 5-1). T-AOC reflects the overall antioxidant capacity of antioxidant factors and antioxidant enzymes. Its concentration was shown in Fig. 5-2A, in which significant differences between control and hypoxia treatment occurred in 1 h and 6 h groups. Overall, the T-AOC change trend was first increased significantly and then returned to the no different level with the control group with the process of hypoxia and reoxygenation. GSH, being composed of glutamic acid, cysteine and glycine, plays an important role in antioxidation and detoxification. The concentration of GSH related factors (T-GSH, GSH, GSSG) were shown in Fig. 5-2B, C, D. Here, Fig. 5-2E showed the ratio of GSH and GSSG (GSH/GSSG) which was more meaningful

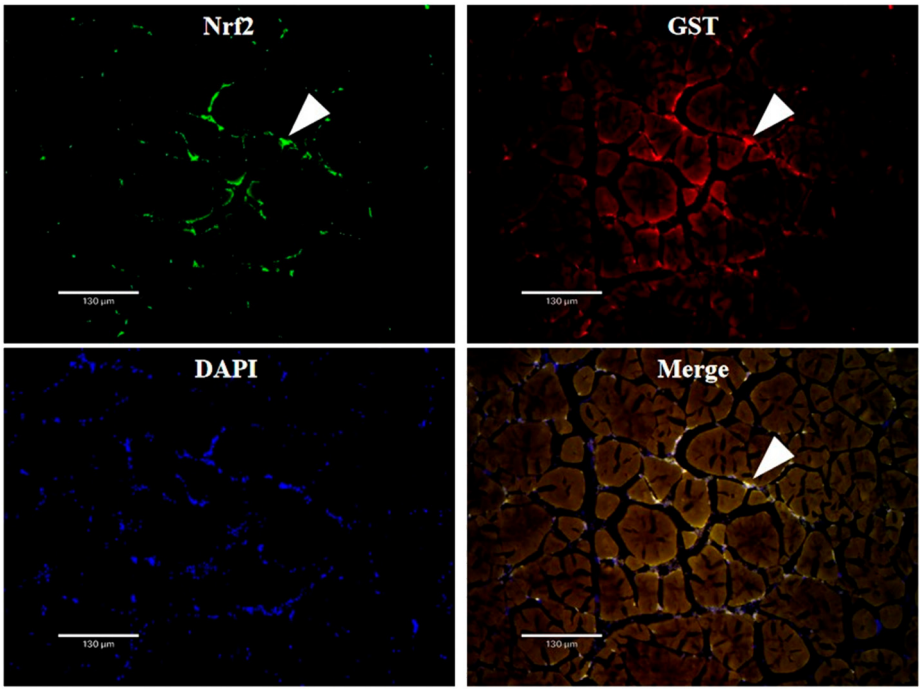

Fig. 4-2. The double in situ hybridization (D-ISH) result of *Nrf2* and *GST* RNAs in skeletal muscle.

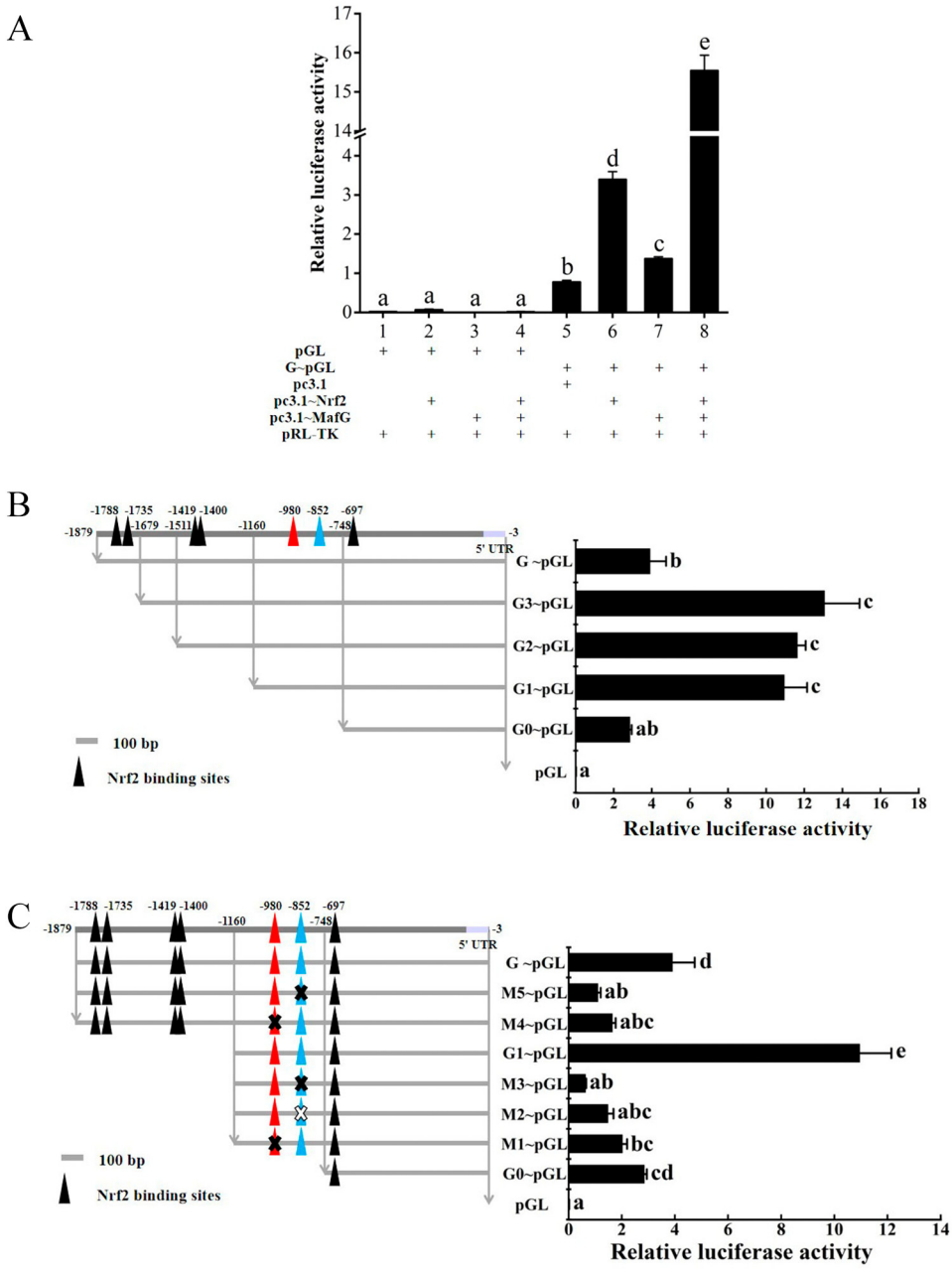

Fig. 4-3. The regulatory relationship of transcription factor Nrf2 on *GST* gene promoter by dual-luciferase reporter assay. (A) The regulation of transcription factor Nrf2 and its partner protein MafG on *GST* gene promoter. pGL and G ~ pGL represent reporter plasmids which were blank (0 bp) circular plasmid pGL 3-Basic and constructed by *GST* gene promoter sequence and fragmented pGL 3-Basic by double restriction endonuclease (*Sac*I and *Hin*dIII), respectively. Pc3.1 and pc3.1 ~ Nrf2, pc3.1 ~ MafG indicate blank circular plasmid pcDNA3.1 (+) and expression plasmids which were constructed by *Nrf2* CDS sequence and fragmented pcDNA3.1 (+) by single restriction endonuclease (BamHI), *MafG* CDS sequence and fragmented pcDNA3.1 (+) by double restriction endonuclease (HindIII and BamHI), respectively. PRL-TK, characterizing the transfection efficiency, is the control plasmid expressing Renilla luciferase (Rluc). Arabic numerals of abscissa in Fig. 4-3A indicate different groups, which 1–5 represent control groups and 6–8 treatment groups. (B) The fragmentation deletion result. The high triangle icons (△) represent the putative Nrf2 binding site. Four different length promoter sequences (G3, G2, G1, G0) are represented by four light gray horizontal lines. G3 ~ pGL, G2 ~ pGL, G1 ~ pGL, G0 ~ pGL were connected by different length *GST* gene promoter sequence and fragmented pGL 3-Basic by double restriction endonuclease (SacI and HindIII), respectively. The construction of G ~ pGL and pGL plasmids are same as that in Fig. 4-3A. (C) The bases mutation result. We mutated two predicted transcription factor binding sites (−980 or −852) to obtain five mutant plasmids (M1 ~ pGL, M2 ~ pGL, M3 ~ pGL, M4 ~ pGL, M5 ~ pGL), which were deleted nearby −980 site putative Nrf2 binding sequence (CAATGTCAG), −852 site putative Nrf2 core binding sequence (GC), −852 site putative Nrf2 binding sequence (GCTGAGTCA), −980 site putative Nrf2 binding sequence (CAATGTCAG), −852 site putative Nrf2 binding sequence (GCTGAGTCA), respectively. The construction of G ~ pGL, G1 ~ pGL, G0 ~ pGL, pGL plasmids are same as that in Fig. 4-3A and B. Different letters indicate significant differences ($P < 0.05$).

to represent the redox state. Their specific change trends were rose first and recovered then, but only T-GSH in R12 h group was significantly higher in hypoxia than in normoxia treatment. CAT, GST and SOD antioxidant enzymes can scavenge ROS by catalyzing their substrates. However, their activities were also not significant except for SOD activity in 12 h time group (Fig. 5-3A, B, C).

4. Discussion

Stress response, an instinct characteristic in life activity, is a defensive behavior to maintain steady state when organism is stimulated. Rapid or slow changes of environmental factors could cause biological stress response, however, organisms have a certain tolerance ability to

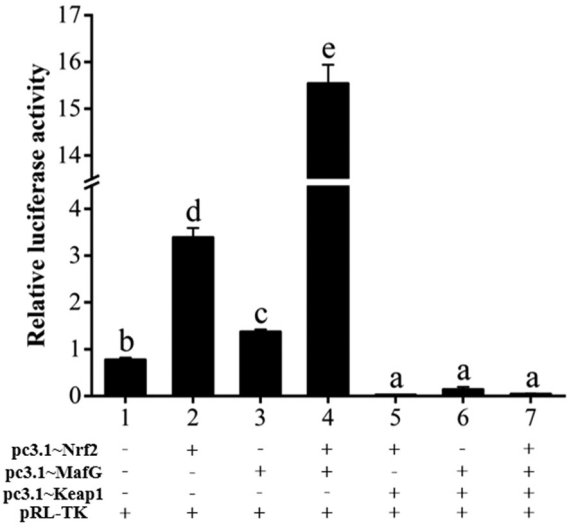

Fig. 4-4. The interaction regulatory relationship of Keap1 with Nrf2 or MafG on *GST* gene promoter by dual-luciferase reporter assay. Pc3.1 ~ Keap1 was constructed by *Keap1* CDS sequence and fragmented pcDNA3.1 (+) by single restriction endonuclease (BamHI). Arabic numerals of abscissa indicate different groups, which 1–4 represent control groups and 5–7 treatment groups. Different letters indicate significant differences ($P < 0.05$).

maintain original physiological activities and phenotype as much as possible (Li et al., 2018; Yang et al., 2017). It is multiple signaling transduction pathways that constitute a signal-transduction network to respond to environmental factors (Nakabayashi and Sasaki, 2005). The protein molecules are often conservative in evolution which was supported by the phylogenetic trees results. So, an important antioxidant signaling pathway of Keap1/Nrf2 (Mafs)-GST, which play a crucial role in human (*Homo sapiens*), house mouse (*Mus musculus*), zebrafish (*Danio rerio*), was noticed in this study to explore the hypoxia tolerance ability of Japanese flounder (Gallego-Selles et al., 2020; Motohashi et al., 2004; Shi and Zhou, 2010). The changes of *Keap1*, *Nrf2* and *GST* expression indicated that this pathway was indeed affected by the DO level of 1.65 mg/L, and the significant effect happened at 3 h. In addition, the results of correlation analyses in expression illustrated that Nrf2 may enhance the expression of *GST* by quantity, while Keap1 is not in this way to *Nrf2*. Keap1 protein usually affect Nrf2 to enter the nucleus by motif binding, so that Nrf2 target gene will not be activated (Kansanen et al., 2013).

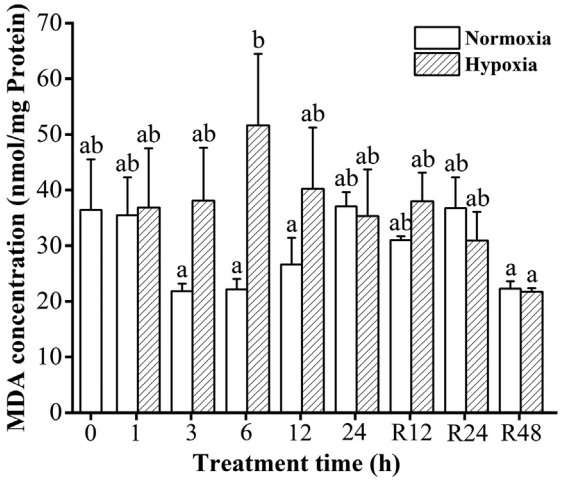

Fig. 5-1. Effect of acute hypoxia on malondialdehyde (MDA) concentration in muscle tissue homogenate. Different letters indicate significant differences ($P < 0.05$).

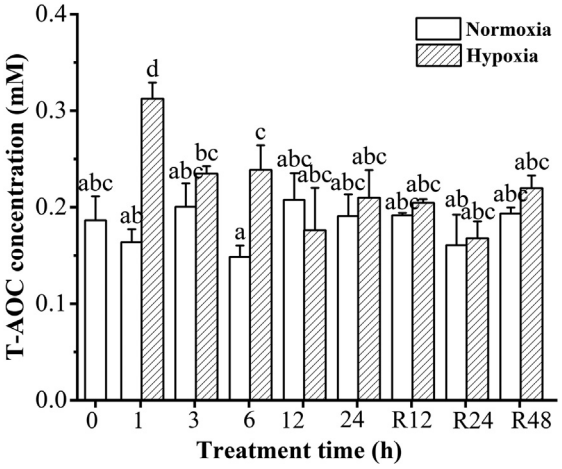

Fig. 5-2A. Effect of acute hypoxia on total antioxidant capacity (T-AOC) in muscle tissue homogenate. Different letters indicate significant differences ($P < 0.05$).

The environmental factors may control epigenetic modification to affect development of organisms (Fan et al., 2020; Sakurada, 2010). Methylation modification, a pattern of epigenetic modification, could effectively influence the expression of *Cosmc*, *Smyd1a*, *Fst*, *cyp19a1a*, *Foxl2* and *Keap1* gene (Huang et al., 2018a; Si et al., 2016; Wang et al., 2008; Wu et al., 2018). In our study, results of the significant decrease of methylation level and the negative correlation between expression and methylation level indicate that hypoxia stress may affect gene expression by changing methylation modification status. Hypomethylation is mainly related to transcriptional activation (Fan et al., 2020). Five negative correlations indicate that their sites (−1941, −1927, −1921, −198 and −169) may be the important regulatory sites, especially −1921 and −169 sites, where methylation status of CpG dinucleotides are strongly negative correlated with the expression level.

Transcription factors can activate gene expression to change biological phenotype. Gilley et al. (2003) found transcription factor FOXO can activate *bim* gene expression to promote apoptosis; TEA domain transcription factor (TEAD) is associated with migration and adhesion of lung cancer (Gao et al., 2019). After confirming the co-existence of *Nrf2* and *GST* in muscle by the D-ISH trial, the activated function of Nrf2 on *GST* gene was investigated. It is concluded from Fig. 4-3A that Nrf2, as a transcription factor, does activate *GST* expression, and the function of Nrf2 dimerization partner MafG is similar to Nrf2 to regulate *GST*. This function of Nrf2 was also confirmed in mice (*Mus musculus*), whose GST and NQO1 enzyme activities were reduced by 50% to 80% in the hepatic and gastric of Nrf2-deficient mice compared that of wild-type mice (Ramos-Gomez et al., 2001). As an antioxidant enzyme, GST can reduce peroxides by catalyzing glutathione peroxidase reactions in antioxidant process (Dixon and Edwards, 2005; Gallagher et al., 2006; Yang et al., 2002). Moreover, the result of relative luciferase activity value is greater when both Nrf2 and MafG expression plasmids coexist indicates that Nrf2 and MafG are synergistic in this pathway. This is consistent with the conclusion that MafS (MafG, MafF) play important roles in the regulation ARE-dependent genes expression (Katsuoka et al., 2005). All these results indicate that MafS and Nrf2 play an important role in the GST related antioxidant process. But our conclusion about MafG is different with that of Rahman et al. (2013) and Motohashi et al. (2004). They thought that MafS contained only binding domain but no active domain, and Nrf2 was necessary for MafG, respectively. Reasons for the difference may be species differences or research methods, so they are worthy to study and discuss further.

To determine the specific binding sites of Nrf2 on *GST* gene promoter, we carried out fragment deletion and base mutation in dual-luciferase reporter assay. According to the Fig. 4-3B, C, it can be

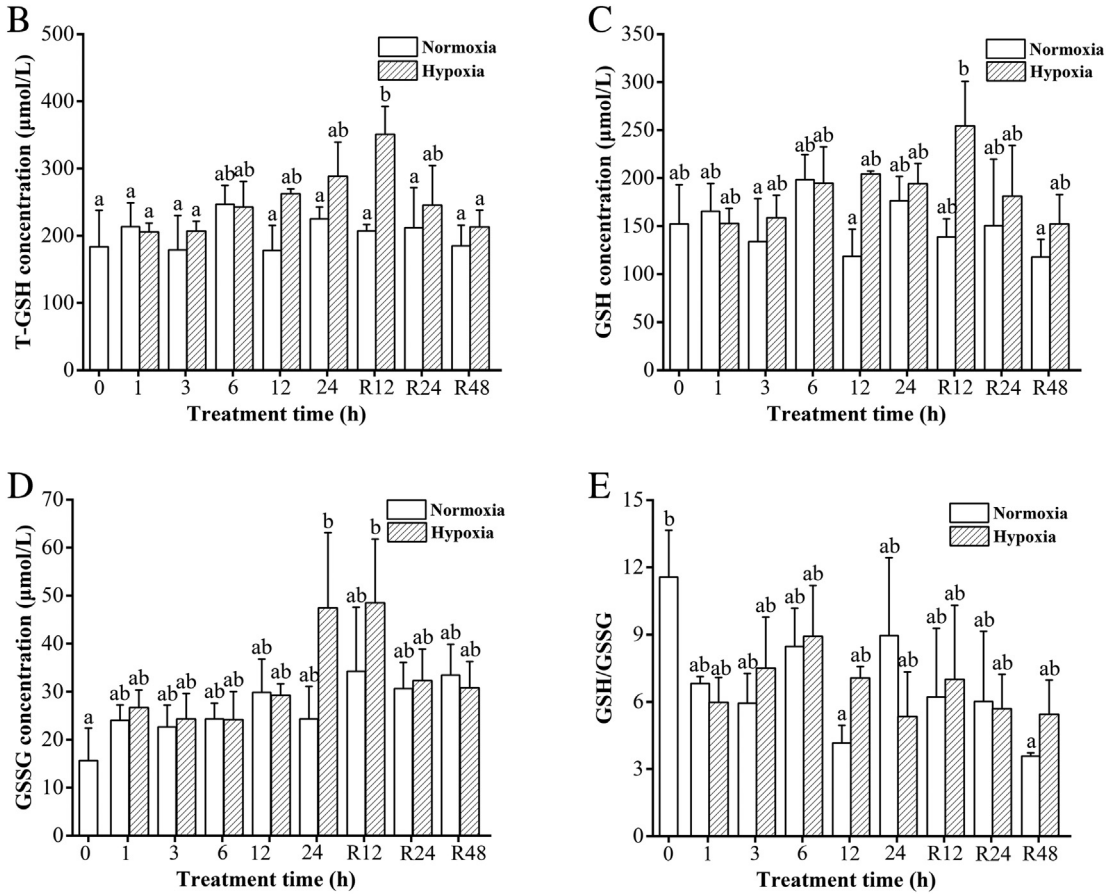

Fig. 5-2. Effects of acute hypoxia on glutathione (GSH) relevant indicators in muscle tissue homogenate. Panels B, C, D, E represent changing trends of total-GSH (T-GSH), GSH, oxidized glutathione (GSSG) and GSH/GSSG with prolongation of hypoxia stress or reoxygenation, respectively. Different letters indicate significant differences ($P < 0.05$).

concluded that the key binding sequences are near −980 site (GCAATG TCA, reverse complementary sequence is TGACATTGC), −852 site (GCTGAGTCA, reverse complementary sequence is TGACTCAGC), in which GC sequence are the more important bases. However, the conclusion is not all consistent with the viewpoint of Hirotsu et al. (2012), who hold that GC dinucleotides are necessary for Nrf2-MafS rather than Nrf2 alone. The significant difference of relative luciferase activity value between G ~ pGL and G1 ~ pGL (d Vs. e) suggests that silencers may exist in the extra sequence (−1879 to −1160 site). In addition, it is proved that Keap1 is an antagonistic factor of Nrf2 (Fig. 4-4), which is a supplement to the expression correlation of *Nrf2* and *Keap1*. Under normoxic condition, Nrf2 protein is anchored and ubiquitinated in the cytoplasm by Keap1, which leads to Nrf2 cannot enter nucleus to perform the transcriptional activation function, and subsequently degraded by the proteasome (McMahon et al., 2003; Mitsuishi et al., 2012). McMahon et al. (2003) also found that Keap1 played negative regulatory function by enhancing Nrf2 degradation rate in proteasomal and altering Nrf2 subcellular distribution. When organism is stimulated, Keap1 will inactivate and release Nrf2, which is not achieved by reducing expression (Mitsuishi et al., 2012). In brief, transcription factor Nrf2 is promoted by MafG and antagonized by Keap1 in the Keap1/Nrf2 (Mafs)-GST pathway.

The trend of MDA changes indicated that muscle cells were damaged when hypoxia occurred. Here, the results of oxidation factors change in skeletal muscle being no significant difference among most groups in our experiment of hypoxia and reoxygenation treatment indicate that the stress response of Japanese flounder to this hypoxia level is not very sensitive. In other words, hypoxia has not significantly affected all these oxidation factors, suggesting that Japanese flounder is a kind of hypoxia tolerant fish. This is consistent with the discovery of larval and juvenile Japanese flounder being hypoxic tolerant (0.2 mg/L) (Ishibashi et al., 2007). Another possible explanation about the results is that the key organ is liver, not skeletal muscle, to balance the redox state (Chatuphonprasert et al., 2013). It is worth mentioning that the concentrations of MDA and T-AOC are significantly different in the 6 h group, indicating that hypoxia stress lasting for 6 h will impact the oxidative metabolism of muscle in Japanese flounder. The recoveries in 12 h group reflect the strong adaptive ability of Japanese flounder. The weak correlation ($R = 0.336$, $R^2 = 0.113$) between GST expression and activity, which were both increased first and then fell, indicated that GST might increase enzyme activity by increasing the amount of GST (Fig. S6). Similarly, the strong adaptive ability may be related to the rapid mobilization of related antioxidant signaling pathways, including Keap1/Nrf2 (Mafs)-GST pathway.

Nrf2 is an important transcription factor to protect cells resist ROS induced oxidative damage (Jiang et al., 2010). The Nrf2 target genes, usually containing ARE sequences in the promoter region, are mainly including anti-injury, anti-stress and anti-drug genes. There are seven ARE sequences in the promoter region of *GST* gene. Previous studies showed that Nrf2-ARE signaling pathway are related with cytoprotection to against carcinogenesis in normal cells (Zhang et al., 2006). Considering many substances, such as (*E*)-N-(2-(3, 5-Dimethoxystyryl) phenyl) furan-2-carboxamide (BK3C231), broccoli seeds and isothiocyanates, olive oil constituent hydroxytyrosol (HT), genistein, can enhance the intensity of this signaling pathway, it is further worth study deeply whether Japanese flounder could enhance resistance and immunity by ingesting these substances (Fan et al., 2016; McWalter et al., 2004; Schaffer and Halliwell, 2011; Tan et al., 2021). The mode of Nrf2 driving function on its target gene may not completely

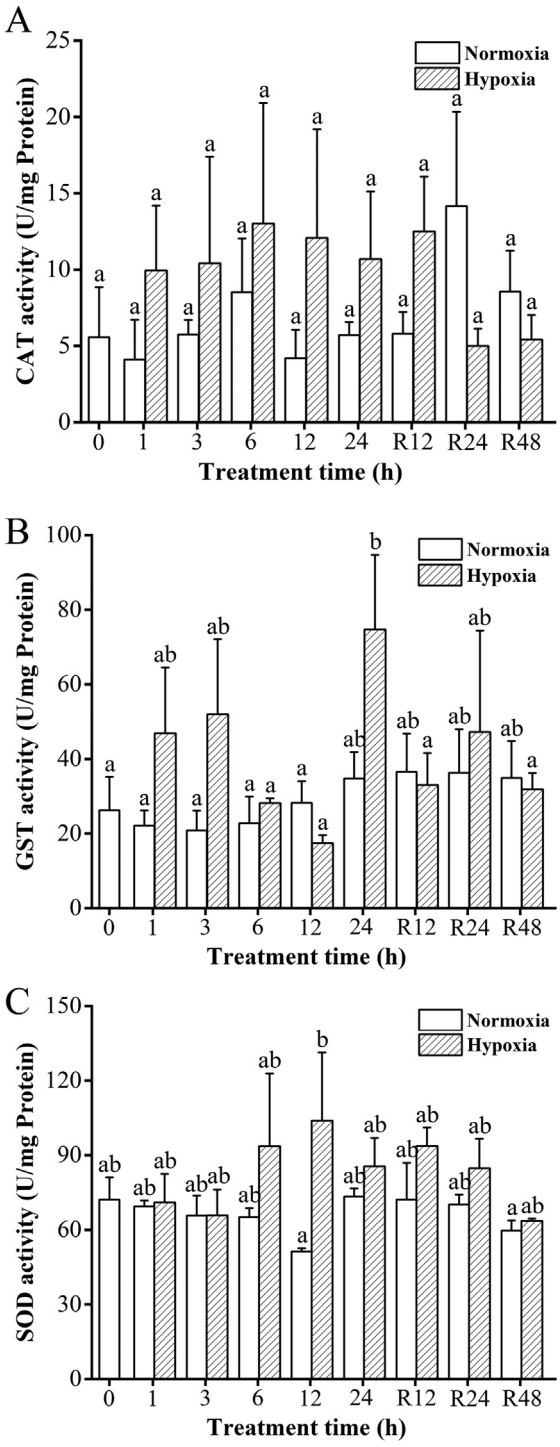

Fig. 5-3. Effects of acute hypoxia on activity of antioxidant enzymes, which include catalase (CAT) (A), glutathione S-transferases (GST) (B) and superoxide dismutase (SOD) (C) in muscle tissue homogenate. Different letters indicate significant differences ($P < 0.05$).

same in different species, and Nrf2 is related with other factors (Notch and AKR1C2) and metabolic process (such as glucose metabolism and amino acid transport) (Hirotsu et al., 2012; Lou et al., 2006; Wakabayashi et al., 2014; Zhang et al., 2006). Furthermore, it is reported that the antioxidative related genes overexpression of Keap1-Nrf2-ARE signaling pathways are related with cancers and carcinogenesis (Mitsuishi et al., 2012; Wang et al., 2008). As a result, further overall research is necessary and essential.

5. Conclusion

The Keap1/Nrf2 (MafG)-GST signaling pathway was enhanced by acute hypoxia stress, which can promote the increase of *GST* expression by upregulating *Nrf2* expression which may be influenced by methylation modification, so the antioxidant capacity was improved in Japanese flounder. In summary, the internal driving force of environmental factors regulation to biological phenotype is signal cascading, which includes epigenetic modification and transcription factor regulation. Taken together, our findings provide new insights (from micro to macro level) into the regulation mechanism of signaling pathway.

CRediT authorship contribution statement

Binghua Liu, Feng He and Haishen Wen conceived and designed the experiments. Binghua Liu, Xiaohui Li, Jun Yang and Guangling Li ran the experiments in laboratory. More specifically, they (Binghua Liu, Xiaohui Li and Jun Yang) reared and sampled fishes, which were also sampled by other members (Xuebin Mao, Donglei Sun, Hongkui Zhao, Jingru Zhang, Xiaojie Wang, Mengqun Liu and Xiaodong Yang et al.) in the laboratory. Subsequently, Binghua Liu detected antioxidant factor (MDA, T-AOC, GSH, SOD, GST, CATMDA, T-AOC, GSH, SOD, GST and CAT) level in muscle tissue homogenate and methylation level of muscle tissue DNA. Binghua Liu and Xiaohui Li performed RNA extractions and q-PCR. Xiaohui Li and Jun Yang conducted the double in situ hybridization. Dual-luciferase reporter assay was performed by Binghua Liu and Guangling Li. Meizhao Zhang, Jifang Li and Feng He revised and approved final version of the manuscript.

Declaration of competing interest

This work was supported by the National Nature Science Foundation of China (31672642), Natural Science Foundation of Shandong Province, China (ZR2014CM018).

There is no conflict of interest in the manuscript, which is approved by all authors for publication. We also declare that the work described is original research that has not been published previously, and not under consideration for publication elsewhere, in whole or in part.

Acknowledgments

This work was supported by the National Nature Science Foundation of China (31672642), Natural Science Foundation of Shandong Province, China (ZR2014CM018).

Appendix A. Supplementary data

Supplementary data to this article can be found online at https://doi.org/10.1016/j.scitotenv.2021.148646.

References

Artner, I., Hang, Y., Mazur, M., Yamamoto, T., Guo, M., Lindner, J., Magnuson, M.A., Stein, R., 2010. MafA and MafB regulate genes critical to β-cells in a unique temporal manner. Diabetes 59, 2530–2539. https://doi.org/10.2337/db10-0190.

Bird, A., 2002. DNA methylation patterns and epigenetic memory. Gene Dev. 16, 6–21. https://doi.org/10.1101/gad.947102.

Blank, V., 2008. Small maf proteins in mammalian gene control: mere dimerization partners or dynamic transcriptional regulators? J. Mol. Biol. 376, 913–925. https://doi.org/10.1016/j.jmb.2007.11.074.

Cabrera, T., Hur, S.B., 2001. The nutritional value of live foods on the larval growth and survival of Japanese flounder, *Paralichthys olivaceus*. J. Appl. Aquac. 11, 35–53. https://doi.org/10.1300/J028v11n01_04.

Canli, Ö., Nicolas, A.M., Gupta, J., Finkelmeier, F., Goncharova, O., Pesic, M., Neumann, T., Horst, D., Löwer, M., Sahin, U., Greten, F.R., 2017. Myeloid cell-derived reactive oxygen species induce epithelial mutagenesis. Cancer Cell 32, 869–883. https://doi.org/10.1016/j.ccell.2017.11.004.

Chatuphonprasert, W., Udomsuk, L., Monthakantirat, O., Churikhit, Y., Putalun, W., Jarukamjorn, K., 2013. Effects of Pueraria mirifica and miroestrol on the

antioxidation-related enzymes in ovariectomized mice. J. Pharm. Pharmacol. 65, 447–456. https://doi.org/10.1111/jphp.12003.
Dixon, D.P., Edwards, R., 2010. Glutathione transferases. The Arabidopsis Book 8, e0131. https://doi.org/10.1199/tab.0131.
Dong, X., Zhang, X., Qin, J., Zong, S., 2013. Acute ammonia toxicity and gill morphological changes of Japanese flounder *Paralichthys olivaceus* in normal versus supersaturated oxygen. Aquac. Res. 44, 1752–1759. https://doi.org/10.1111/j.1365-2109.2012.03181.x.
Duan, Y., Dong, X., Zhang, X., Miao, Z., 2011. Effects of dissolved oxygen concentration and stocking density on the growth, energy budget and body composition of juvenile Japanese flounder, *Paralichthys olivaceus* (Temminck et Schlegel). Aquac. Res. 42, 407–416. https://doi.org/10.1111/j.1365-2109.2010.02635.x.
Evans, P.M., Zhang, W., Chen, X., Yang, J., Bhakat, K.K., Liu, C., 2007. Krüppel-like factor 4 is acetylated by p300 and regulates gene transcription via modulation of histone acetylation. J. Biol. Chem. 282, 33994–34002. https://doi.org/10.1074/jbc.M701847200.
Everis, L., Betts, G., 2001. pH stress can cause cell elongation in *Bacillus* and *Clostridium* species: a research note. Food Control 12, 53–56. https://doi.org/10.1016/S0956-7135(00)00017-7.
Fan, Y., Wei, W., Luo, J., Jin, Y., Dai, Z., 2016. Genistein promotes the metabolic transformation of acetaminophen to glucuronic acid in human L-O2, HepG2 and Hep3b cells *via* the Nrf2/Keap1 pathway. Food Funct. 7, 4683–4692. https://doi.org/10.1039/c6fo00889e.
Fan, X., Hou, T., Guan, Y., Li, X., Zhang, S., Wang, Z., 2020. Genomic responses of DNA methylation and transcript profiles in zebrafish cells upon nutrient deprivation stress. Sci. Total Environ. 722, 137980. https://doi.org/10.1016/j.scitotenv.2020.137980.
Fuji, K., Hasegawa, O., Honda, K., Kumasaka, K., Sakamoto, T., Okamoto, N., 2007. Marker-assisted breeding of a lymphocystis disease-resistant Japanese flounder (*Paralichthys olivaceus*). Aquaculture 272, 291–295. https://doi.org/10.1016/j.aquaculture.2007.07.210.
Gallagher, E.P., Gardner, J.L., Barber, D.S., 2006. Several glutathione S-transferase isozymes that protect against oxidative injury are expressed in human liver mitochondria. Biochem. Pharmacol. 71, 1619–1628. https://doi.org/10.1016/j.bcp.2006.02.018.
Gallego-Selles, A., Martin-Rincon, M., Martinez-Canton, M., Perez-Valera, M., Martín-Rodríguez, S., Gelabert-Rebato, M., Santana, A., Morales-Alamo, D., Dorado, C., Calbet, J.A.L., 2020. Regulation of Nrf2/Keap1 signalling in human skeletal muscle during exercise to exhaustion in normoxia, severe acute hypoxia and post-exercise ischaemia: influence of metabolite accumulation and oxygenation. Redox Biol. 36, 101627. https://doi.org/10.1016/j.redox.2020.101627.
Gao, R., Yun, Y., Cai, Z., Sang, N., 2019. $PM_{2.5}$-associated nitro-PAH exposure promotes tumor cell metastasis through Hippo-YAP mediated transcriptional regulation. Sci. Total Environ. 678, 611–617. https://doi.org/10.1016/j.scitotenv.2019.04.420.
Gilley, J., Coffer, P.J., Ham, J., 2003. FOXO transcription factors directly activate *bim* gene expression and promote apoptosis in sympathetic neurons. J. Cell Biol. 162, 613–622. https://doi.org/10.1083/jcb.200303026.
Hirotsu, Y., Katsuoka, F., Funayama, R., Nagashima, T., Nishida, Y., Nakayama, K., Douglas Engel, J., Yamamoto, M., 2012. Nrf2–MafG heterodimers contribute globally to antioxidant and metabolic networks. Nucleic Acids Res. 40, 10228–10239. https://doi.org/10.1093/nar/gks827.
Huang, Y., Hu, N., Si, Y., Li, S., Wu, S., Zhang, M., Wen, H., Li, J., Li, Y., He, F., 2018a. Methylation status of the *Follistatin* gene at different development stages of Japanese Flounder (*Paralichthys olivaceus*). J. Ocean Univ. China 17, 1243–1252. https://doi.org/10.1007/s11802-018-3712-6.
Huang, Y., Wen, H., Zhang, M., Hu, N., Si, Y., Li, S., He, F., 2018b. The DNA methylation status of *MyoD* and *IGF-I* genes are correlated with muscle growth during different developmental stages of Japanese flounder (*Paralichthys olivaceus*). Comp. Biochem. Physiol. B 219-220, 33–43. https://doi.org/10.1016/j.cbpb.2018.02.005.
Innamorato, N.G., Rojo, A.I., García-Yagüe, Á.J., Yamamoto, M., Ceballos, M.L.d., Cuadrado, A., 2008. The transcription factor Nrf2 is a therapeutic target against brain inflammation. J. Immunol. 181, 680–689. https://doi.org/10.4049/jimmunol.181.1.680.
Ishibashi, Y., Kotaki, T., Yamada, Y., Ohta, H., 2007. Ontogenic changes in tolerance to hypoxia and energy metabolism of larval and juvenile Japanese flounder *Paralichthys olivaceus*. J. Exp. Mar. Biol. Ecol. 352, 42–49. https://doi.org/10.1016/j.jembe.2007.06.036.
Ishii, S., Nakao, S., Minamikawa-Tachino, R., Desnick, R.J., Fan, J.-Q., 2002. Alternative splicing in the α-galactosidase a gene: increased exon inclusion results in the fabry cardiac phenotype. Am. J. Hum. Genet. 70, 994–1002. https://doi.org/10.1086/339431.
Jiang, T., Huang, Z., Lin, Y., Zhang, Z., Fang, D., Zhang, D.D., 2010. The protective role of Nrf2 in streptozotocin-induced diabetic nephropathy. Diabetes 59, 850–860. https://doi.org/10.2337/db09-1342.
Kanda, S., Okubo, K., Oka, Y., 2011. Differential regulation of the luteinizing hormone genes in teleosts and tetrapods due to their distinct genomic environments - insights into gonadotropin beta subunit evolution. Gen. Comp. Endocrinol. 173, 253–258. https://doi.org/10.1016/j.ygcen.2011.05.015.
Kansanen, E., Kuosmanen, S.M., Leinonen, H., Levonen, A.L., 2013. The Keap1-Nrf2 pathway: mechanisms of activation and dysregulation in cancer. Redox Biol. 1, 45–49. https://doi.org/10.1016/j.redox.2012.10.001.
Kaspar, J.W., Niture, S.K., Jaiswal, A.K., 2009. Nrf2:INrf2 (Keap1) signaling in oxidative stress. Free Radic. Biol. Med. 47, 1304–1309. https://doi.org/10.1016/j.freeradbiomed.2009.07.035.
Katsuoka, F., Motohashi, H., Ishii, T., Aburatani, H., Engel, J.D., Yamamoto, M., 2005. Genetic evidence that small maf proteins are essential for the activation of antioxidant response element-dependent genes. Mol. Cell. Biol. 25, 8044–8051. https://doi.org/10.1128/MCB.25.18.8044-8051.2005.
Ke, B., Shen, X.D., Zhang, Y., Ji, H., Gao, F., Yue, S., Kamo, N., Zhai, Y., Yamamoto, M., Busuttil, R.W., Kupiec-Weglinski, J.W., 2013. Keap1-Nrf2 complex in ischemia-induced hepatocellular damage of mouse liver transplants. J. Hepatol. 59, 1200–1207. https://doi.org/10.1016/j.jhep.2013.07.016.
Lee, J.M., Calkins, M.J., Chan, K., Kan, Y.W., Johnson, J.A., 2003. Identification of the NF-E2-related factor-2-dependent genes conferring protection against oxidative stress in primary cortical astrocytes using oligonucleotide microarray analysis. J. Biol. Chem. 278, 12029–12038. https://doi.org/10.1074/jbc.M211558200.
Li, X., Deng, S.-j., Zhu, S., Jin, Y., Cui, S.-p., Chen, J.-y., Xiang, C., Li, Q.-y., He, C., Zhao, S.-f., Chen, H.-y., Niu, Y., Liu, Y., Deng, S.-c., Wang, C.-y., Zhao, G., 2016. Hypoxia-induced lncRNA-NUTF2P3-001 contributes to tumorigenesis of pancreatic cancer by derepressing the miR-3923/KRAS pathway. Oncotarget 7, 6000–6014. https://doi.org/10.18632/oncotarget.6830.
Li, M., Wang, X., Qi, C., Li, E., Du, Z., Qin, J.G., Chen, L., 2018. Metabolic response of Nile tilapia (*Oreochromis niloticus*) to acute and chronic hypoxia stress. Aquaculture 495, 187–195. https://doi.org/10.1016/j.aquaculture.2018.05.031.
Li, Q., Wen, H., Li, Y., Zhang, Z., Wang, L., Mao, X., Li, J., Qi, X., 2020. FOXO1A promotes neuropeptide FF transcription subsequently regulating the expression of feeding-related genes in spotted sea bass (*Lateolabrax maculatus*). Mol. Cell. Endocrinol. 517, 110871. https://doi.org/10.1016/j.mce.2020.110871.
Lin, L., Kragh, P.M., Purup, S., Kuwayama, M., Du, Y., Zhang, X., Yang, H., Bolund, L., Callesen, H., Vajta, G., 2009. Osmotic stress induced by sodium chloride, sucrose or trehalose improves cryotolerance and developmental competence of porcine oocytes. Reprod. Fert. Develop. 21, 338–344. https://doi.org/10.1071/RD08145.
Lou, H., Du, S., Ji, Q., Stolz, A., 2006. Induction of *AKR1C2* by phase II inducers: identification of a distal consensus antioxidant response element regulated by Nrf2. Mol. Pharmacol. 69, 1662–1672. https://doi.org/10.1124/mol.105.019794.
Lu, Y., Nie, M., Wang, L., Xiong, Y., Wang, F., Wang, L., Xiao, P., Wu, Z., Liu, Y., You, F., 2018. Energy response and modulation of AMPK pathway of the olive flounder *Paralichthys olivaceus* in low-temperature challenged. Aquaculture 484, 205–213. https://doi.org/10.1016/j.aquaculture.2017.11.031.
McMahon, M., Itoh, K., Yamamoto, M., Hayes, J.D., 2003. Keap1-dependent proteasomal degradation of transcription factor Nrf2 contributes to the negative regulation of antioxidant response element-driven gene expression. J. Biol. Chem. 278, 21592–21600. https://doi.org/10.1074/jbc.M300931200.
McWalter, G.K., Higgins, L.G., McLellan, L.I., Henderson, C.J., Song, L., Thornalley, P.J., Itoh, K., Yamamoto, M., Hayes, J.D., 2004. Transcription factor Nrf2 is essential for induction of NAD(P)H: Quinone Oxidoreductase 1, Glutathione S-Transferases, and Glutamate Cysteine Ligase by Broccoli seeds and isothiocyanates. J. Nutr. 12, 3499S. https://doi.org/10.1093/jn/134.12.3499S.
Mitsuishi, Y., Taguchi, K., Kawatani, Y., Shibata, T., Nukiwa, T., Aburatani, H., Yamamoto, M., Motohashi, H., 2012. Nrf2 redirects glucose and glutamine into anabolic pathways in metabolic reprogramming. Cancer Cell 22, 66–79. https://doi.org/10.1016/j.ccr.2012.05.016.
Miyazaki, T., Seikai, T., Kinoshita, I., Tsukamoto, K., 2004. Comparison of escape behavior of wild and hatchery-reared juvenile Japanese flounder *Paralichthys olivaceus*. Fish. Sci. 70, 7–10. https://doi.org/10.1111/j.1444-2906.2003.00763.x.
Motohashi, H., Katsuoka, F., Engel, J.D., Yamamoto, M., 2004. Small Maf proteins serve as transcriptional cofactors for keratinocyte differentiation in the Keap1-Nrf2 regulatory pathway. PNAS 101, 6379–6384. https://doi.org/10.1073/pnas.0305902101.
Nakabayashi, J., Sasaki, A., 2005. Optimal phosphorylation step number of intracellular signal-transduction pathway. J. Theor. Biol. 233, 413–421. https://doi.org/10.1016/j.jtbi.2004.10.022.
Nordberg, J., Arnér, E.S.J., 2001. Reactive oxygen species, antioxidants, and the mammalian thioredoxin system. Free Radical Bio. Med. 31, 1287–1312. https://doi.org/10.1016/S0891-5849(01)00724-9.
Overgaard, J., Gesser, H., Wang, T., 2007. Tribute to P. L. Lutz: cardiac performance and cardiovascular regulation during anoxia/hypoxia in freshwater turtles. J. Exp. Biol. 210, 1687–1699. https://doi.org/10.1242/jeb.001925.
Rahman, M.M., Sykiotis, G.P., Nishimura, M., Bodmer, R., Bohmann, D., 2013. Declining signal dependence of Nrf2-MafS-regulated gene expression correlates with aging phenotypes. Aging Cell 12, 554–562. https://doi.org/10.1111/acel.12078.
Ramos-Gomez, M., Kwak, M.-K., Dolan, P.M., Itoh, K., Yamamoto, M., Talalay, P., Kensler, T.W., 2001. Sensitivity to carcinogenesis is increased and chemoprotective efficacy of enzyme inducers is lost in *nrf2* transcription factor-deficient mice. PNAS 98, 3410–3415. https://doi.org/10.1073/pnas.051618798.
Rytkönen, K.T., Vuori, K.A.M., Primmer, C.R., Nikinmaa, M., 2007. Comparison of hypoxia-inducible factor-1 alpha in hypoxia-sensitive and hypoxia-tolerant fish species. Comp. Biochem. Phys. D 2, 177–186. https://doi.org/10.1016/j.cbd.2007.03.001.
Sakurada, K., 2010. Environmental epigenetic modifications and reprogramming-recalcitrant genes. Stem Cell Res. 4, 157–164. https://doi.org/10.1016/j.scr.2010.01.001.
Schaffer, S., Halliwell, B., 2011. Comment on hydroxytyrosol induces proliferation and cytoprotection against oxidative injury in vascular endothelial cells: role of Nrf2 activation and HO-1 induction. J. Agric. Food Chem. 59, 10770–10771. https://doi.org/10.1021/jf201509k.
Seikai, T., Tanangonan, J.B., Tanaka, M., 1986. Temperature influence on larval growth and metamorphosis of the Japanese flounder *Paralichthys olivaceus* in the laboratory. Bull. Jpn. Soc. Sci. Fish. 52, 977–982. https://doi.org/10.2331/suisan.52.977.
Shi, X., Zhou, B., 2010. The role of Nrf2 and MAPK pathways in PFOS-induced oxidative stress in zebrafish embryos. Toxicol. Sci. 115, 391–400. https://doi.org/10.1093/toxsci/kfq066.
Shinozaki, K., Yamaguchi-Shinozaki, K., 2007. Gene networks involved in drought stress response and tolerance. J. Exp. Bot. 58, 221–227. https://doi.org/10.1093/jxb/erl164.
Shu, Y., Tao, Y., Wang, S., Huang, L., Yu, X., Wang, Z., Chen, M., Gu, W., Ma, H., 2015. *GmSBH1*, a homeobox transcription factor gene, relates to growth and development and involves in response to high temperature and humidity stress in soybean. Plant Cell Rep. 34, 1927–1937. https://doi.org/10.1007/s00299-015-1840-7.

Si, Y., Ding, Y., He, F., Wen, H., Li, J., Zhao, J., Huang, Z., 2016. DNA methylation level of *cyp19a1a* and *Foxl2* gene related to their expression patterns and reproduction traits during ovary development stages of Japanese flounder (*Paralichthys olivaceus*). Gene 575, 321–330. https://doi.org/10.1016/j.gene.2015.09.006.

Singer, D., 1999. Neonatal tolerance to hypoxia: a comparative-physiological approach. Comp. Biochem. Phys. A 123, 221–234. https://doi.org/10.1016/s1095-6433(99)00057-4.

Sykiotis, G.P., Bohmann, D., 2010. Stress-activated cap'n'collar transcription factors in aging and human disease. Sci. Signal. 3, re3. https://doi.org/10.1126/scisignal.3112re3.

Tan, H.H., Thomas, N.F., Inayat-Hussain, S.H., Chan, K.M., 2021. (E)-N-(2-(3, 5-Dimethoxystyryl) phenyl) furan-2-carboxamide (BK3C231) induces cytoprotection in CCD18-Co human colon fibroblast cells through Nrf2/ARE pathway activation. Sci. Rep. 11, 4773. https://doi.org/10.1038/s41598-021-83163-7.

Tian, Y., Wen, H., Qi, X., Zhang, X., Li, Y., 2019. Identification of *mapk* gene family in *Lateolabrax maculatus* and their expression profiles in response to hypoxia and salinity challenges. Gene 684, 20–29. https://doi.org/10.1016/j.gene.2018.10.033.

Wakabayashi, N., Skoko, J.J., Chartoumpekis, D.V., Kimura, S., Slocum, S.L., Noda, K., Palliyaguru, D.L., Fujimuro, M., Boley, P.A., Tanaka, Y., Shigemura, N., Biswal, S., Yamamoto, M., Kensler, T.W., 2014. Notch-Nrf2 axis: regulation of *Nrf2* gene expression and cytoprotection by Notch signaling. Mol. Cell. Biol. 34, 653–663. https://doi.org/10.1128/MCB.01408-13.

Wang, R., An, J., Ji, F., Jiao, H., Sun, H., Zhou, D., 2008. Hypermethylation of the *Keap1* gene in human lung cancer cell lines and lung cancer tissues. Biochem. Biophys. Res. Co. 373, 151–154. https://doi.org/10.1016/j.bbrc.2008.06.004.

Wang, H., Tang, X., Xing, J., Sheng, X., Chi, H., Zhan, W., 2021. Effect of raising water temperature on proliferation of hirame novirhabdovirus (HIRRV) and antiviral response of olive flounder (*Paralichthys olivaceus*). Aquaculture 540, 736751. https://doi.org/10.1016/j.aquaculture.2021.736751.

Wu, S., Huang, Y., Li, S., Wen, H., Zhang, M., Li, J., Li, Y., Shao, C., He, F., 2018. DNA methylation levels and expression patterns of *Smyd1a* and *Smyd1b* genes during Metamorphosis of the Japanese Flounder (*Paralichthys olivaceus*). Comp. Biochem. Physiol. B 223, 16–22. https://doi.org/10.1016/j.cbpb.2018.05.002.

Yan, J., Pang, Y., Zhuang, J., Lin, H., Zhang, Q., Han, L., Ke, P., Zhuang, J., Huang, X., 2019. Selenepezil, a selenium-containing compound, exerts neuroprotective effect via modulation of the Keap1-Nrf2-ARE pathway and attenuates Aβ-induced cognitive impairment in vivo. ACS Chem. Neurosci. 10, 2903–2914. https://doi.org/10.1021/acschemneuro.9b00106.

Yang, Y., Sharma, R., Zimniak, P., Awasthi, Y.C., 2002. Role of α class glutathione S-transferases as antioxidant enzymes in rodent tissues. Toxicol. Appl. Pharmacol. 182, 105–115. https://doi.org/10.1006/taap.2002.9450.

Yang, S., Yan, T., Wu, H., Xiao, Q., Fu, H.M., Luo, J., Zhou, J., Zhao, L.L., Wang, Y., Yang, S.Y., Sun, J.L., Ye, X., Li, S.J., 2017. Acute hypoxic stress: effect on blood parameters, antioxidant enzymes, and expression of *HIF-1alpha* and *GLUT-1* genes in largemouth bass (*Micropterus salmoides*). Fish Shellfish Immun. 67, 449–458. https://doi.org/10.1016/j.fsi.2017.06.035.

Zhang, J., Ohta, T., Maruyama, A., Hosoya, T., Nishikawa, K., Maher, J.M., Shibahara, S., Itoh, K., Yamamoto, M., 2006. BRG1 interacts with Nrf2 to selectively mediate *HO-1* induction in response to oxidative stress. Mol. Cell. Biol. 26, 7942–7952. https://doi.org/10.1128/MCB.00700-06.